25th ABCM International Congress of Mechanical Engineering
October 20-25, 2019, Uberlândia, MG, Brazil

THERMAL ANALYSIS OF A PARABOLIC TROUGH COLLECTOR

Fernanda Ignácio Nascimento
Elí Wilfredo Zavaleta-Aguilar
São Paulo State University (Unesp), Campus of Itapeva, Rua Geraldo Alckmin, 519, 18409-010 Itapeva, São Paulo, Brazil.
fernanda.ignacio@unesp.br
eli.zavaleta@unesp.br

Abstract. *This work constitutes the thermal analysis of parabolic trough solar collector (PTC) in order to obtain its necessary geometry as function, mainly, of the required thermal load and temperature. For this, a mathematical model was developed and an algorithm for numerical simulation performed in Matlab® software, was generated. The model was tested with theoretical and experimental studies getting a PTC length maximum deviation of 7.44 %. In addition, it was analyzed the PTC geometry sensitivity according to vacuum condition, solar radiation, heat transfer fluid mass flow rate, thermal load, reflector width and heat transfer fluid type. Finally, the model was applied to a 1 RT ammonia-water absorption refrigeration cycle obtaining a necessary length of 11.7 m for 1 m reflector width.*

Keywords: *Solar trough collector, solar energy, thermal modeling, absorption refrigeration cycle.*

1. INTRODUCTION

Parabolic trough solar collectors constitute a mature commercial solar thermal technology. They are used extensively in concentrating solar power, solar industrial heating processes, solar chemistry, solar desalination and solar cooling (Xu et al., 2019). Such devices are proposed for applications requiring intermediate concentration rates and temperatures in the range of 100 ºC to 400°C (Duffie and Beckman, 2013).

PTCs are basically constituted of a parabolic structure covered by a reflective sheet material which reflect the direct radiation reaching on its surface to a focal line where the receiver (also called absorber) is located. The receiver is basically a metal tube externally coated with selective material that absorbs the concentrated radiation, transforms it in useful heat and transmits it to a heat transfer fluid (HTF) that circulates inside. Generally, the metal tube is inserted into a glass tube. PTCs generally have a tracking mechanism system, which orient it in an east-west direction, tracking the sun from north to south or in a north to south direction, tracking the sun from east to west (Kalogirou, 2012).

The PTC reflector parabolic geometry is directly related to the receiver diameter ($D_{3,calc}$) according to Eq. (1) and (2) (Kalogirou, 2016).

$$D_{3,calc}=2\left(\frac{2f}{1+\phi_r}\right)\sin 0.267 \tag{1}$$

$$w=4f\tan\left(\frac{\phi_r}{2}\right) \tag{2}$$

Where, f is the focal length, ϕ_r the rim angle and w the PTC width. It was noted that the receiver external diameter used in experimental and numerical works (D_3) do not follow the Eq. (1) and (2) as shown in Tab. 1. This table indicates that the external receiver diameter used and the theoretical one ratio ($D_3/D_{3,calc}$) varies from 1.38 to 13.63, and the glass cover internal diameter and receiver external diameter used ratio (D_4/D_3) varies from 1.45 to 1.85.

The rim angle (ϕ_r) is defined as the angle between the axis and the line from the focus to the edge of the concentrator and it is recommended to be 70° and 110° (Gunther, Joemann, and Csambor, 2010). According to Kalogirou (2016) a rim angle of 90° causes that the average focal-reflector distance and thus the reflected beam dispersion is minimized, so the inclination and tracking errors are smaller.

On the other side, the cold production through absorption refrigeration systems has been traditionally considered one of the most desirable applications for solar thermal energy (Li, Zhang and Yang, 2015). A solar refrigeration system consists basically on the use of absorption refrigeration cycles (ARC) in combination with solar thermal systems to produce the cooling effect (Musbah et al., 2014), requiring little or no electrical input (Kim and Ferreira, 2008). The working fluids conventionally used in these cycles are lithium bromide – water (LiBr/ H_2O) and ammonia – water (NH_3/H_2O) pairs (Flores, Román and Alpírez, 2014). The ARCs have four main components, which are: the generator, the condenser, the evaporator and the absorber. The energy that drives this cooling system, in this case, is the parabolic trough solar collector, which feeds the generator.

Table 1. Reflector geometry and absorber and glass cover diameters.

Authors	f (m)	ϕ_r (°)	w (m)	r_r (m)	D_2 (m)	D_3 (m)	D_4 (m)	D_5 (m)	$D_{3,\,calc}$ (m)	$\frac{D_3}{D_{3,\,calc}}$	$\frac{D_4}{D_3}$
Mokhtaria et al. (2007)	0.880	90.0	3.4	1.760		0.070		0.125	0.016	4.267	
Valan-arasu and Sornakumar (2007)	0.200	90.0	0.80	0.400		0.013		0.023	0.004	3.434	
Gomes and Guedes (2010)	0.400	70.0	0.50	0.596	0.014	0.015			0.006	2.700	
Sauceda et al. (2011)	0.750	90.0	3	1.500	0.020	0.027	0.045	0.050	0.014	1.910	1.685
Venegas-Reyes et al. (2012)	0.716	45.0	1.187	0.839		0.025			0.008	3.249	
Macedo-Valencia et al. (2014)	0.112	96.0	0.5	0.250		0.013			0.002	5.447	
Tzivanidis et al. (2015)	0.300	70.0	0.84	0.447	0.020	0.022	0.032	0.034	0.004	5.281	1.455
Bhujangrao (2016)	0.221	134.5	1.03	1.479	0.017	0.019			0.012	1.378	
Ismail, Zanardi and Lino (2016)	0.100	90.0		0.200		0.025	0.047	0.05	0.002	13.627	1.850
Tijani and Jamarei (2016)	1.840	68.4	5	2.689	0.065	0.070	0.109	0.115	0.025	2.793	1.557
Bharti and Paul (2017)	0.447	80.0	1.5	0.762	0.021	0.025			0.007	3.579	
Pavlovic et al. (2017)	1.840	68.4	5	2.689	0.066	0.070	0.110	0.115	0.025	2.793	1.571
Qu et al. (2017)	1.710	80.3	5.77	2.927	0.064	0.070	0.114	0.120	0.027	2.566	1.629
Abbood, Radhi and Shaheed (2018)	0.233	77.7	0.75	0.384		0.047		0.058	0.007	13.118	
Lamrani et al. (2018)	1.840	49.6	3.4	2.233	0.066	0.070	0.109	0.115	0.021	3.364	1.557
Xu et al. (2019)	1.710	80.2	5.76	2.923	0.064	0.070	0.119	0.125	0.027	2.570	

This work aims to evaluate the parabolic through solar collector geometry for a given practical application. In addition, it will be analyzed the sensitivity of PTC geometry as function of relevant variables, also, it will be applied the numerical simulation to size a PTC for an ammonia-water absorption refrigeration cycle (AARC) as function of its thermal load, the operating temperature, among other variables. This study is relevant since there is not work in the literature that lead with sizing a parabolic trough collector as function of a specific thermal application.

2. METHODOLOGY

The parabolic trough solar collector analyzed here has four main surfaces (2, 3, 4 and 5 as shown in Fig. (1)) that will be considered in the energy balance between the heat transfer fluid inside the receiver and the environment. Figure 1 shows the PTC cross section indicating its main parts: the reflector, the receiver, the glass cover and the heat transfer fluid (HTF). In this figure, one can see that the direct solar radiation impacts the reflector and a portion of it is reflected reaching the glass cover first, then the receiver, being $\dot{Q}_{5,abs}$ and $\dot{Q}_{3,abs}$ the radiation absorbed by those, respectively. At the receiver, the heat is transferred from surface 3 to surface 2 by conduction ($\dot{Q}_{32,cond}$) and then to the HTF by convection ($\dot{Q}_{21,conv}$). Heat losses occur from surface 3 to surface 4 by convection ($\dot{Q}_{34,conv}$) and radiation ($\dot{Q}_{34,rad}$), then from surface 4 to surface 5 the heat loss is transferred by conduction $\left(\dot{Q}_{34,cond}\right)$. From surface 5, heat is lost to environment (6) by convection ($\dot{Q}_{56,conv}$) and radiation $\dot{Q}_{56,rad}$. The energy balances (first law of thermodynamics) were determined considering permanent regime and kinetic and potential energy fluid variation negligible. Thus, the energy balances on surface 5, 4, 3 and 2 correspond to Eq. (2), (3), (4) and (5), respectively.

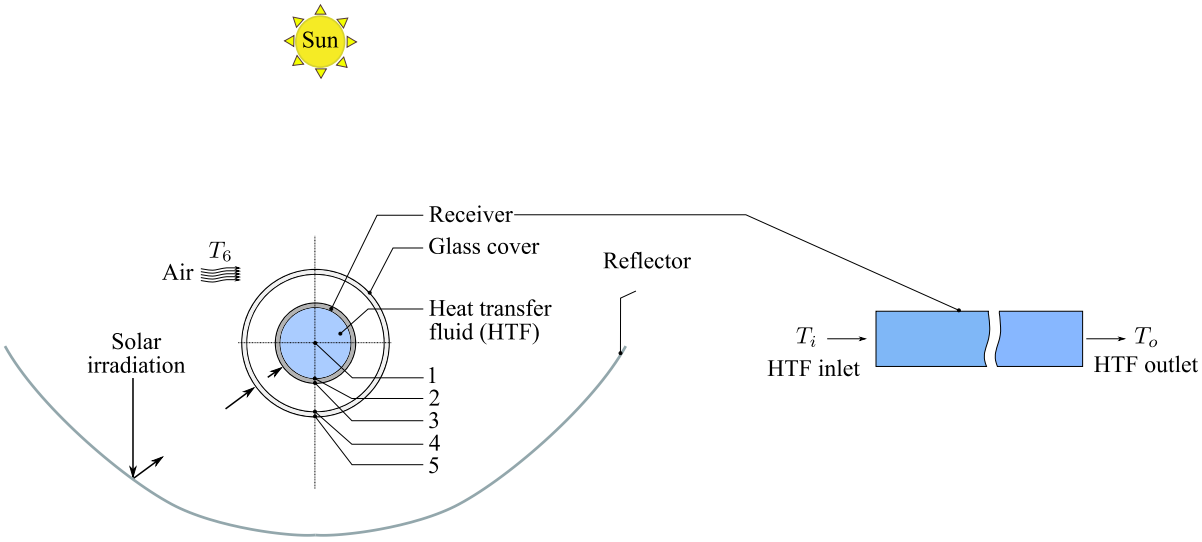

Figure 1. Schematic of the parabolic trough solar collector.

$$\dot{Q}_{5,abs} + \dot{Q}_{45,cond} = \dot{Q}_{56,rad} + \dot{Q}_{56,conv} \tag{3}$$

$$\dot{Q}_{34,rad} + \dot{Q}_{34,conv} = \dot{Q}_{45,cond} \tag{4}$$

$$\dot{Q}_{3,abs} = \dot{Q}_{32,cond} + \dot{Q}_{34,rad} + \dot{Q}_{34,conv} \tag{5}$$

$$\dot{Q}_{32,cond} = \dot{Q}_{21,conv} = \dot{Q}_u \tag{6}$$

Where, $\dot{Q}_u$ is the useful heat gain transferred to the heat transfer fluid (W), also, evaluated by the First Law of Thermodynamics between the inlet and outlet heat transfer fluid at the receiver, as follow:

$$\dot{Q}_u = \dot{m} c_p (T_o - T_i) \tag{7}$$

In the previous equation, $\dot{m}$ is the HTF mass flow rate (kg/s), c_p is the HTF thermal capacity (J/kgK) and T_o and T_i are HTF outlet and inlet temperatures (K) respectively.

2.1 Simplifications

Some simplifications are proposed to reduce negligible parameters. On surface 3 the absorbed solar irradiation ($\dot{Q}_{3,abs}$) is considered constant along its diameter and length. On surface 5, the absorbed radiation is considered negligible ($\dot{Q}_{5,abs} \approx 0$). On surfaces 4 and 5 it is assumed that conduction occurs on a thin wall, with no significant temperature

variation ($T_4 \approx T_5$). At the annular region (between surfaces 3 and 4), if the pressure is bigger than 0.013 Pa, the convection heat transfer between the receiving tube and the glass cover ($\dot{Q}_{34,conv}$) occurs by natural convection, otherwise, if this pressure is less than 0.013 Pa, the convection is disregarded ($\dot{Q}_{34,conv} \approx 0$), since it is assumed that there is vacuum in this region (Kalogirou, 2012).

The sky temperature is considered similar to that of the environment to calculate the heat transfer by radiation from the glass cover to the sky. One-dimension model (1D) in the radial direction is assumed for Eqs. (3) to (6), and the surface temperatures are considered approximately constant. The radiation absorbed by the receiver is defined as:

$$\dot{Q}_{3,abs} = SA \tag{8}$$

Where A is the collector opening area (m^2) and S is the radiation absorbed by the receiver per collector opening area unit (W/m^2), defined by Eq. (9):

$$S=\eta_{opt} I \tag{9}$$

In Eq. (9), I is direct solar radiation (W/m^2) and η_{opt} optical efficiency is given by:

$$\eta_{opt}= \rho\tau_5\alpha_3\gamma K \tag{10}$$

Where ρ is the reflector reflectivity, τ_5 is the glass cover transmittivity, α_3 is the receiver absorptivity, γ is the intercept factor, which represents the rays fraction incident upon the aperture area that reach the receiver and K is the incidence angle modifier, which quantifies the effect of the incidence angle on the parameters: ρ, τ_5, α_3 and γ.

By combining equations of surface 2, it is possible to obtain the useful heat gain:

$$\dot{Q}_u = \frac{T_3 - 0.5(T_o+T_i)}{\frac{ln\left(\frac{D_3}{D_2}\right)}{2\pi k_3 L} + \frac{1}{\pi D_2 L h_f}} \tag{11}$$

In the previous relation, T_3 is the receiver external temperature (K), D_2 is the receiver internal diameters (m), respectively, k_3 is the receiver thermal conductivity (W/mK), L is the PTC length (m) and h_f is the HTF convection heat transfer coefficient (W/m^2K), that is evaluated through the Nusselt number:

$$Nu_f= \frac{h_f D_2}{k_f} \tag{12}$$

If the flow is in laminar condition, (Re_f < 2300) the Nusselt number is Nu = 4.36, for turbulent condition flow (Re_f > 10000) the Nusselt number is defined follow the Dittus-Boelter equation:

$$Nu_f=0.023 Re_f^{0.8} Pr^{0.4} \tag{13}$$

In the Eq. (12), k_f is the HTF thermal conductivity (W/mK) and in Eq. (13), Pr and Re are the Prandtl and Reynolds numbers, respectively, the last one defined as:

$$Re_f= \frac{4\dot{m}}{\pi D_2 \mu_f} \tag{14}$$

Where μ_f is the HTF dynamic viscosity (kg/ms). By combining Eq. (3) and Eq. (4), one obtains:

$$\frac{D_3\sigma(T_3^4 - T_5^4)}{\frac{1}{\varepsilon_3} + \frac{D_3}{D_4}\left(\frac{1 - \varepsilon_5}{\varepsilon_5}\right)} = \varepsilon_5 D_5 \sigma\left(T_5^4 - T_6^4\right) + D_5 h_w (T_5 - T_6) - \frac{2k_{eff}(T_3 - T_5)}{ln\frac{D_4}{D_3}} \tag{15}$$

In the previous equation, σ is the Boltzmann's constant (5.67 x 10-8 W/m2K4), ε_3 and ε_5 are the receiver and glass cover emissivity, respectively, D_5 is the glass cover external diameters (m), h_w is the external air convection heat transfer coefficient (W/m^2K), T_5 is the external glass cover temperature (K), T_6 is the ambient temperature (K) and k_{eff} is the effective heat transfer coefficient for natural convection in the annular region (W/mK). If vacuum is considered, the term $2k_{eff}(T_3 - T_5)/ln(D_4/D_3)$ must be disregarded.

The h_w coefficient can be estimated as follow (Kalogirou, 2016):

$$Nu_w = \frac{h_w D_5}{k_w} \tag{16}$$

For $0.1 < Re_w < 1000$,

$$Nu_w = 0.4 + 0.54 Re^{0.52} \tag{17}$$

For $1000 < Re_w < 50000$,

$$Nu_w = 0.3 Re_w^{0.6} \tag{18}$$

$$Re_w = \frac{\rho_w V D_5}{\mu_w} \tag{19}$$

Where k_w, ρ, μ and V are the thermal conductivity, density, dynamic viscosity and velocity of the air, respectively. The effective heat transfer coefficient k_{eff} is obtained by (Raithby and Hollands, 1975):

$$k_{eff} = 0.386 k_a \left(\frac{Pr_a}{0.861 + Pr_a} \right)^{1/4} Ra_c^{1/4} \tag{20}$$

In the previous relation, k_a, Pr_a and Ra_c are the thermal conductivity, Prandtl number and Rayleigh number of the air, respectively, evaluated at surface 3 and 4 average temperature.

By combining Eq. (5) and (6), yields:

$$SL(w - D_5) = \dot{Q}_u + \frac{\pi D_3 L \sigma (T_3^4 - T_5^4)}{\frac{1}{\varepsilon_3} + \frac{D_3}{D_4}\left(\frac{1 - \varepsilon_5}{\varepsilon_5}\right)} + \frac{2\pi L k_{eff}(T_3 - T_5)}{ln\frac{D_4}{D_3}} \tag{21}$$

If vacuum is considered the term $2\pi L k_{eff}(T_3 - T_5)/ln(D_4/D_3)$ must be disregarded.

Finally, the PTC thermal efficiency is defined as the useful heat gain and the radiation incident upon the aperture area ratio:

$$\eta = \frac{\dot{Q}_u}{I A} \tag{22}$$

2.2 Simulation

Given the nonlinear Eqs. (7) to (21), an algorithm was implemented in Matlab Mathworks® software to evaluate the variables L, T_i, T_3, e T_5. The algorithm flowchart is shown in Fig. 2. In the first iteration, the temperature T_5 was adjusted to be one-degree Kelvin greater than that of the ambient.

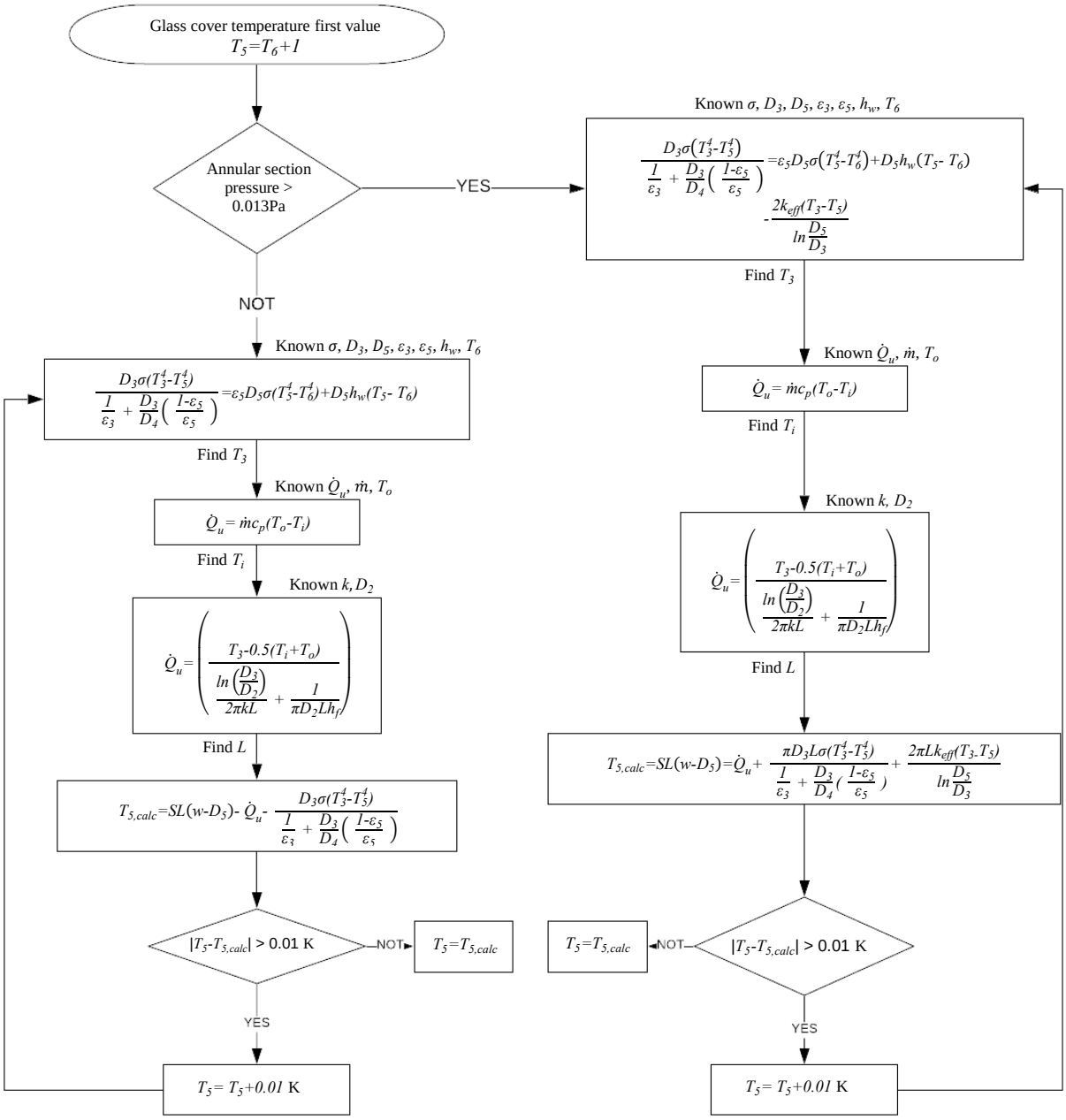

Figure 2. Algorithm flowchart scheme.

3. RESULTS AND DISCUSSIONS

3.1 Comparison with the literature

The algorithm was compared with one experimental (Sagade, Aher e Shinde, 2013) and two (Marif et al., 2014 and Kalogirou, 2016) analytical works. The required input variables are: D_2, D_3, D_4, D_5, ε_3, ε_5, ρ, τ_5, α_3, γ, K, w, I, S, k_3, T_o, $\dot{m}$, c_p and V, giving as result: the collector length (L), the absorber temperature (T_3) and the glass cover temperature (T_5). The results are shown in Tab. 2. It can be seen in this table that the length collector relative deviation was 0.83 to 7.44 %, for the receiver temperature 0.04 to 16.27 % and for the glass cover 1.80 to 2.66 %.

Table 2. Comparison with the literature.

Variables	A Sagade, Aher e Shinde (2013)	This work	Marif et al. (2014)	This work	Kalogirou (2016)	This work	Variation of the error (%)
L (m)	1.21	1.22	7.80	8.38	20.00	20.62	0.83 - 7.44
T_3 (K)	342.15	342.00	449.15	522.21	533.00	549.38	0.04 - 16.27
T_5 (K)	-	314.52	341.15	332.07	337.00	343.05	1.80 - 2.66

3.2 Parameter sensitivity analysis

In this section, it was analyzed the sensitivity of some relevant PTC parameters. For this, it was used the following input variables: D_2 = 0.040 m, D_3 = 0.050 m, D_5 = 0.090 m, ε_3 = 0.92, ε_5 = 0.87, ρ = 0.935, τ_5 = 0.89, α_3 = 0.93, γ = 0.95, K = 1, w = 1 m, I = 680.08 W/m^2, k_3 = 15 W/mK, T_o = 546.6 K, $\dot{m}$ = 0.32 kg/s and V = 5 m/s, it was used Therminol® VP-1 as HTF. The analysis was made considering all the variables constant and varying only the variable of interest to verify its influence on the PTC length and thermal efficiency. The parameters analyzed were: direct solar radiation (I), mass flow rate ($\dot{m}$), useful heat gain ($\dot{Q}_u$) and PTC width (w) which are shown in Fig. 3. In addition, the PTC length sensitivity was analyzed as function of the HTF output temperature (T_o) and the HTF type fluid (Therminol® VP-1, Therminol® 59, water and thermo-solar salt 40% KNO_3 60% $NaNO_3$), this result is shown in Fig. 4.

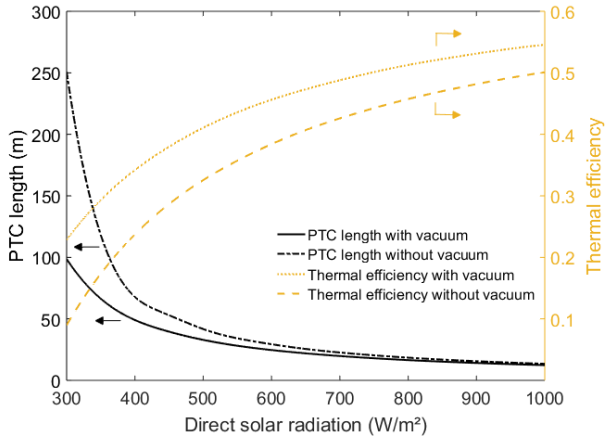

(a) Influence of the direct solar radiation.

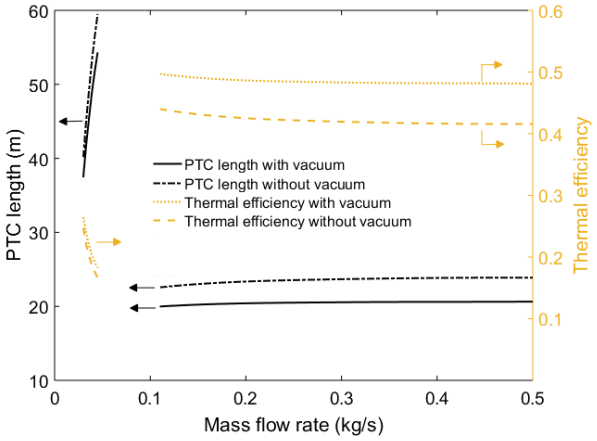

(b) Influence of the HTF mass flow rate.

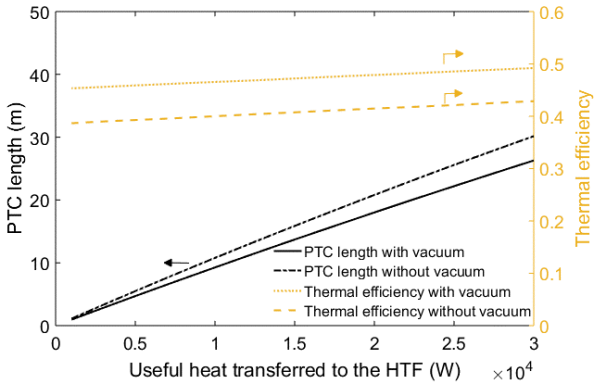

(c) Influence of the useful heat gain.

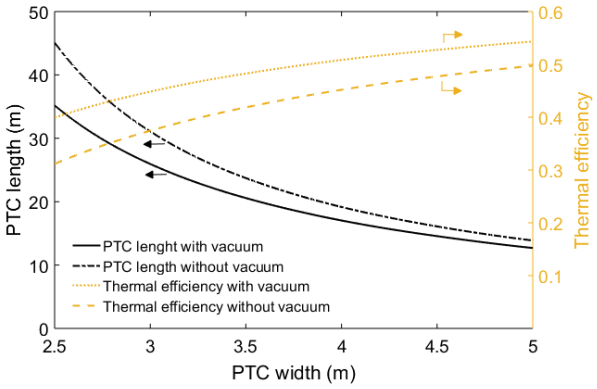

(d) Influence of the PTC width.

Figure 3. PTC length and thermal efficiency sensitivity as function of (a) direct solar radiation, (b) HTF mass flow rate, (c) useful heat gain and (d) PTC width for Therminol ® VP-1 fluid.

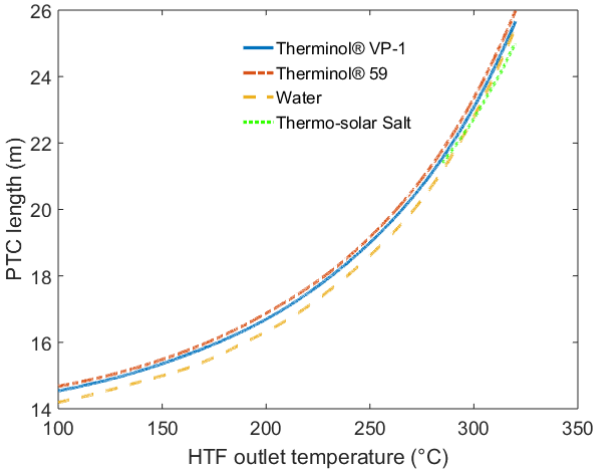

Figure 4. PTC length sensitivity in relation to HTF output temperature and several work fluids.

It can be seen in Fig. 3 (a), (b), (c) and (d) that when non-evacuated annular region between the receiver and the glass cover is assumed, the collector length is bigger. This behavior is justified because the convection thermal losses in this region.

In Fig. 3 (a) it is noted that the increase of the direct solar radiation leads to decrease the PTC length. In addition, the lower the direct solar radiation, the greater the PTC length difference between the annular vacuum and non-vacuum condition. This may be due to a smaller difference T_3^4 - T_5^4 (Eq. (21)) in non-vacuum situation for low solar direct radiation However, when the radiation reaches around 700 W/m^2, the collector length becomes gradually shorter and the vacuum and non-vacuum lengths have approximately the same value. It can also be noted that the thermal efficiency for vacuum condition is higher due to the thermal losses are smaller than non-vacuum condition.

Figure 3 (b) shows that PTC length initially increases with the HTF mass flow rate in laminar condition. After, approximately at 0.11 kg/s, in turbulent condition, the PTC length begins to rise slightly and then becomes nearly constant (from 0.3 kg/s). The interval between 0.045 kg/s and 0.11 kg/s represents the transient flow state and it is not considered in the graph. It is also verified that the thermal efficiency follows the inverse behavior of the collector length for the laminar flow state, but for the turbulent flow it does not vary significantly.

In Fig. 3 (c) it is observed that the PTC length for vacuum and non-vacuum conditions start approximately with the same value and as the useful heat gain increases, they move apart, following an increment approximately linear. This may be due to the smaller difference T_3^4 - T_5^4, as mentioned in Fig. 3 (a). It is also noticed that for vacuum situation the thermal efficiency is higher, because in non-vacuum situation there is the thermal losses by convection.

In Fig. 3 (d) it is observed that the PTC length varies inversely to its width. For smaller PTC width the difference between the collector lengths for vacuum and non-vacuum is bigger. Such a difference is related to the smaller difference T_3^4 - T_5^4 for smaller width values, resulting in the same situation as commented in Fig 3 (a). The thermal efficiency, for non-vacuum condition is lower due to bigger thermal losses occurring in the non-evacuated region.

Figure 4 illustrates the PTC length behavior as function of HTF. All HTF are considered to be in liquid condition. The temperature (T_o) range for Thermo-solar salt in liquid condition (260°C-593°C) starts at 285°C, differing to others HTF that begin in 100 °C. The PTC length behavior of Therminol® VP-1 and Therminol® 59 are very similar because their thermophysical properties do not vary considerably. PTC working with water gets shorter PTC length compared to the other fluids. The necessary PTC length for Thermo-solar salt is closer to water than to the other two fluids.

3.3 Sizing a PTC for an ammonia-water absorption refrigeration cycle

The proposed algorithm was applied to size a PTC for a 1 RT ammonia-water absorption refrigeration cycle. According to Zavaleta-Aguilar (2015a) the *COP* (coefficient of performance) of this cycle is approximately 0.52 so it is necessary $\dot{Q}_u$ = 6763.3 W to drive this AARC. The necessary temperature to promote the ammonia-water separation into the distiller is around 373 K to 408 K which depends on the solution concentration, solution mass flow rate, among others (Zavaleta-Aguilar, 2015b).

For dimensioning the PTC it was established ϕ_r = 90° and w = 1 m. From Eqs. (1) and (2) one can obtain f = 0.25 m and $D_{3,calc}$ = 0.0047 m, this value will be incremented in 4.5 times (according to Tab. 1), giving as result D_3 = 0.0207 m. It was chosen a receiver thickness of 1 mm, so D_2 = 0.0187 m. The glass cover internal diameter is shown to be 1.6 times D_3 (according to Tab. 1) so D_4 = 0.0331 m. A glass cover thickness of 0.0028 m, gives as result D_5 = 0.0387 m. Other parameters are: ε_3 = 0.92, ε_5 = 0.87, ρ = 0.935, τ_5 = 0.89, α_3 = 0.93, γ = 0.95, K = 1, w = 1 m, I = 900 W/m^2, k_3 = 15 W/mK,

T_6 = 298.15 K, T_o = 408 K, $\dot{m}$ = 0.8426 kg/s and V = 5 m/s. The HTF considered is Therminol® 59. The results of the simulation are shown in Tab. 3.

Table 3. Results for the ARC.

Variable description	Variable	With vacuum	Without vacuum
PTC lenght	L (m)	11.66	12.59
HTF inlet temperature	T_i (K)	404.08	404.08
Receiver temperature	T_3 (K)	409.83	409.55
Glass cover temperature	T_5 (K)	318.63	311.51

4. CONCLUSION

The proposed model was satisfactory considering the complexity of the equations involved, getting as maximum length relative error of 7.44 %. Sensitivity analysis of PTC showed that the receiver and the glass cover temperatures are determinant for the collector sizing, as well as, the vacuum condition in the annular region between the receiver and the glass cover. In addition, Fig. 3 (b) showed that the laminar or turbulent flow condition influences directly the collector length and, consequently, on its thermal efficiency. It was also possible to verify the thermal efficiency behavior as function of some project variables. This model can be used to evaluate the geometry of any parabolic collector as a function, mainly, of the thermal load, the required operating temperatures, among others.

5. REFERENCES

Abbood, M.H., Radhi, R.M. and Shaheed, A.A., 2018. "Design, construction, and testing of a parabolic trough solar concentrator system for hot water and moderate temperature steam generation". *Kufa Journal of Engineering*, Vol. 9, No. 1, pp. 42-59.

Bharti, A. and Paul, B., 2017. "Design of solar parabolic trough collector". In *Procedings of the International Conference on Advances in Mechanical, Industrial, Automation and Management Systems – AMIAMS 2017.* Allahabad, India.

Bhujangrao, K.H., 2016. "Design and development of prototype cylindrical parabolic solar collector for water heating application". *International Journal of Renewable Energy Development*, Vol. 5, No. 1, pp. 49-55.

Duffie, J.A. and Beckman, W.A., 2013. *Solar engineering of thermal processes*. John Wiley & Sons, New Jersey, 4th edition.

Flores, V.H.; Román, J.C. and Alpírez, G.M., 2012. "Performance analysis of different working fluids for an absorption refrigeration cycle". *American Journal of Environmental Engineering*, Vol. 4, pp. 1-10.

Gomes, M.A. and Guedes, G.P., 2010. "Development of a Parabolic Cylindric Solar Concentrator for Fluid Heating". *In Proceedings of the 3nd Brazilian Congress of Solar Energy – 2010*. Belém, Brazil.

Gunther, M., Joemann, M. and Csambor, S. 2010. "Parabolic Trough Technology", Advanced CSP Teaching Materials, pp. 1-106.

Ismail, K.A.R., Zanardi, M.A. and Lino, F. A. M., 2016. "Modeling and validation of a parabolic solar collector with a heat pipe absorber." *Advances in Energy Research*, Vol. 4, No. 4, pp. 299-323.

Kalogirou, S.A., 2012. "A detailed thermal model of a parabolic trough collector receiver". *Energy*, Vol. 48, pp. 298-306.

Kalogirou, S.A., 2016. Engenharia de energia solar. Elsevier, Rio de Janeiro, 2nd edition.

Kim, D.S., Ferreira, C.A., 2008. "Solar refrigeration options – a state-of-the-art review". *International Journal of Refrigeration*, Vol. 31, No. 1, pp. 3-15.

Lamrani, B., Khouya, A., Zeghmati, B. and Draoui, A., 2018. "Mathematical modeling and numerical simulation of a parabolic trough collector: A case study in thermal engineering". *Thermal Science and Engineering Progress*, Vol. 8, pp. 47-54.

Li, H., Zhang, X. and Yang, C., 2015. "Analysis on All-Day Operating Solar Absorption Refrigeration System with Heat Pump System" *Procedia Engineering*, Vol. 121, pp. 349-356.

Macedo-Valencia, J., Ramírez-Ávila, J., Acosta, R., Jaramillo, O. A. and Aguilar, J. O., 2014. "Design, construction and evaluation of parabolic trough collector as demonstrative prototype". *Energy Procedia*, Vol. 57, pp. 989-998.

Marif, Y., Benmoussa, H., Bouguettaia, H., Belhadj, M. and Zerrouki, M., 2014. "Numerical simulation of solar parabolic trough collector performance in the Algeria Saharan region". *Energy Conversion And Management*, Vol. 85, pp. 521-529.

Mokhtaria., A., Yaghoubi, M., Kanan, P., Vadiee, A. and Hessami R., 2007. "Thermal and Optical Study af Parabolic Trough Collectors of Shiraz Solar Power Plant". *In Procedings of the Third International Conference on Thermal Engineering: Theory and Applications – 2007*. Amman, Jordan.

Musbah, M., Zivkovic, B.D., Kosi, F.F., Abdulgalil, M.M. and Sretenovic, A.A., 2014. "Solar energy contribution to the energy demand for air conditioning system in an office building under Tripoli climate conditions". *Thermal Science*, Vol. 18, No. 1, pp. 1-12.

Pavlovic, S., Bellos, E., Stefanovic, V. and Tzivanidis, C., 2017. "Optimum geometry of parabolic trough collectors with optical and thermal criteria". *International Review of Applied Sciences and Engineering*, Vol. 8, No. 1, pp. 45-50.

Qu, W., Wang, R., Hong, H., Sun J. and Jin, H., 2017. "Prototype testing of a 300kWth solar parabolic-trough collector using rotatable axis tracking". *Energy Procedia*, Vol. 105, pp. 780-786.

Raithby, G.D., and Hollands, K.G.T., 1975. "A general method of obtaining approximate solutions to laminar and turbulent free convection problems". *Advances in Heat Transfer*, Vol. 11, pp. 265-315.

Sagade, A., Aher, S., and Shinde, N.N., 2013. "Performance evaluation of low-cost FRP parabolic trough reflector with mild steel receiver". *International Journal Of Energy And Environmental Engineering*, Vol. 4, No. 1, pp. 5-13.

Sauceda, D., Velázquez, N., García-Valladares, O. and Beltrán, R., 2011. "Numerical simulation and design of a parabolic trough solar collector used as a direct generator in a solar-GAX cooling cycle. *Journal of Mechanical Science and Technology*, Vol. 25, No. 6, pp. 1399-1408.

Tijani, A.S. and Jamarei, M.J.B., 2016. "Numerical Investigation of Thermal Losses from Air Filled Annulus of a Parabolic Trough Solar Collector". *Journal of Mechanical Engineering*, Vol. 13. No. 2, pp. 1-15.

Tzivanidis, C., Bellos, E., Korres, D., Antonopoulos, K.A. and Mitsopoulos, G., 2015. "Thermal and optical efficiency investigation of a parabolic trough collector". *Case Studies in Thermal Engineering*, Vol. 6, pp. 226-237.

Valan-Arasu, A. and Sornakumar, T., 2007. "Theoretical analysis and experimental verification of parabolic trough solar collector with hot water generation system". *Thermal Science*, Vol. 11, No. 1, pp. 119-126.

Venegas-Reyes, E., Jaramillo, O.A., Castrejón-García, R., Aguilar, J.O. and Sosa-Montemayor, F., 2012. "Design, construction, and testing of a parabolic trough solar concentrator for hot water and low enthalpy steam generation". *Journal Of Renewable And Sustainable Energy*, Vol. 4, No. 5, pp. 1-19.

Xu, L., Sun, F., Ma, L., Li, X., Lei, D., Yuan, G., Zhu, H., Zhang, Q., Xu, E. and Wang, Z., 2019. "Analysis of optical and thermal factors' effects on the transient performance of parabolic trough solar collectors". *Solar Energy*, Vol. 179, pp.195-209.

Zavaleta-Aguilar, E.W., 2015a. *Estudo experimental de um destilador por filme descendente para um ciclo de refrigeração por absorção de amônia-água em um banco de tubos horizontais*. Ph.D. thesis, Universidade de São Paulo, São Paulo, Brazil.

Zavaleta-Aguilar, E.W., Simões-Moreira, J.R., 2015b. "Horizontal tube bundle falling film distiller for ammonia–water mixtures", *International Journal of Refrigeration*, Vol. 59, pp. 304–316.

6. RESPONSIBILITY NOTICE

The authors are the only responsible for the printed material included in this paper.